

## **FILTERING SARS-COV-2 VIRUS AEROSOLS WITH NEW ELECTRET NANOFIBER FILTER**

Wallace Leung<sup>1</sup>, Qiangqiang Sun<sup>1</sup>

<sup>1</sup>The Hong Kong Polytechnic University, Hong Kong

Corresponding Author: [Wallace.leung@polyu.edu.hk](mailto:Wallace.leung@polyu.edu.hk)

***Proceeding for the WFC13, Oct 6-9, 2022, San Diego, CA, USA***

**Keywords:** Charged multilayer PVDF nanofiber filter, filter testing, ambient and sodium chloride aerosols, SARS-CoV-2 virus (COVID-19), facemask and respirator

### **ABSTRACT**

The SARS-CoV-2 virus leading to COVID-19 pandemic, average size 100 nm, can be aerosolized by coughing, sneezing, talking, and even breathing from an infected person. The aerosol carrier for the virus can be tiny droplets and particulates from an infected person, fine suspended mists in air, or ambient aerosols. Unfortunately, there are no test standards for nano-aerosols less than 100 nm. Our goal is to develop air filters for personal protective equipment with 90% capture for 100-nm ambient aerosols with pressure drop less than 30 Pa at face velocity of 5.3 cm/s. There are two challenges. First, this airborne bio-nanoaerosol (virus and carrier) is amorphous unlike cubic NaCl crystals. Second, unlike standard laboratory tests on NaCl and test oil droplets, the polydispersed aerosols challenge the filter simultaneously and they can interact complicating the filtration testing process. For the first time, we have studied these two effects using ambient aerosols simulating the bio-nanoaerosols of coronavirus challenging charged multilayer nanofiber filters. This problem is complicated due to mechanical and electrostatic interactions among aerosols of different sizes with induced charges of different magnitudes. The test filters were arranged in 2, 4, and 6 multiple-layers stack-up with each layer having 0.765 g/m<sup>2</sup> of charged PVDF nanofibers. This configuration also minimized electrical interference among neighboring charged nanofibers and reduced flow resistance in the filter. For ambient aerosol size > 80 nm and depending on the number of layers in the filter, the electrostatic effect contributes 100%–180% more efficiency to the existing mechanical efficiency due primarily to diffusion and interception capture. By stacking-up layers to increase fiber basis weight in the filter, a 6-layer charged nanofiber filter achieved 88%, 88% and 96% filtration efficiency for, respectively, 55-nm, 100-nm and 300-nm ambient aerosol. The pressure drop for the 6-layer nanofiber filter was only 26 Pa (2.65 mm water column). The quality factor is between 0.1 and 0.13 Pa<sup>-1</sup>. Using the same filter, laboratory tests results using monodispersed NaCl aerosols of 50, 100, and 300 nm yielded filtration efficiency, respectively, 92%, 94% and 98% (qualified for 'N98 standard') with same pressure drop of 26 Pa. The 6-layer charged PVDF nanofiber filter provides good personal protection against airborne coronavirus virus and nanoaerosols based on the "N98 standard", yet 10X more breathable than a conventional N95 or FFP2 respirator.

# 1. INTRODUCTION

## 1.1 Background

The major transmission mechanism of the novel coronavirus (or SARS-CoV-2) is airborne. This explains the wide spread of the latest virus variant Omicron with incredible infection rate that shocked the entire world catching people off-guard. The virus can be attached to aerosols emitting from an index subject (infected person) through breathing, coughing, sneezing, singing, and talking. The aerosol can be a particulate or a respiratory droplet. During winter season with low relative humidity, less than 50%, the respiratory droplet can evaporate reducing further in size by as much as 10 times [1]. This also explains why influenza is so widespread during the dry winter months. Of course, another factor is that the virus can survive longer in colder environment. When the aerosol size reduces to less than 5 microns, the aerosol stays in the air and does not settle practically at all. Aerosols breathing out from an infected person can be readily inhaled by person passing by in fleeting moments of 5-10 seconds [1]. When people are inadequately protected (not wearing or wearing low-protective masks) and when the level of the breathed out from an infected person has high viral load (*Cycle Threshold for PCR tests* <20), the infected person can infect at least 20 people. Further, Omicron variant virus has a high infection rate on the upper respiratory track once it enters the human body affecting seriously elderly and small children. This explains the wide-spread transmission of the Omicron variant of the virus and thus the COVID-19 disease since November 2021.

Fig. 1a shows schematically a coronavirus of size 60-140 nm [2] being attached to a carrier aerosol. For a small coronavirus, the virus plus the aerosol carrier overall size is still small. On the other hand, when the virus is attached to a larger carrier aerosol, the overall size can be similar in size as the carrier aerosol, see Fig. 1b. Thus, the range of aerosol size is between 60 – 300 nm similar in size of smoke particles emitted from burning incense and smoking cigarette. In fact, a good example to demonstrate whether the facemask provides adequate protection is to find out if the facemask wearer can smell smoke when passing by a person smoking a cigarette within a 2-meter distance [1].

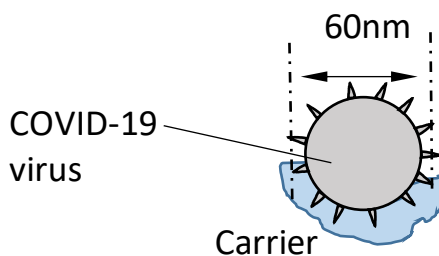


Fig. 1a - Coronavirus attached to a carrier of similar size or smaller and become airborne. The resulting aerosol is about 60 nm.

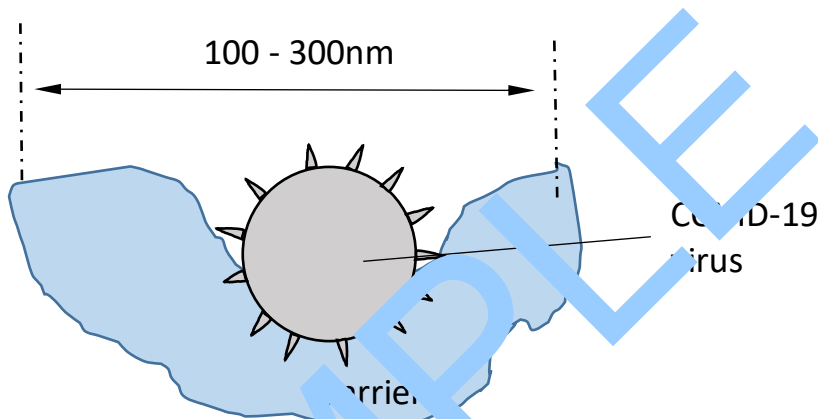


Fig. 1b - Coronaviruses (60-140 nm) attached to a carrier of larger size and become airborne. The resulting aerosol may be 100 to 300 nm.

All conventional face masks are made of melt-blown electret microfibers. The diameter of the fibers is  $6 \pm 3 \mu\text{m}$ . It is known that the electric force varies as inversely proportional to the separation distance between a charged pole (or fiber) and a charged particle. When the fiber diameter is reduced from  $6 \mu\text{m}$  to  $0.3 \mu\text{m}$ , the electric force can be enhanced tremendously. The above description is applicable to charged aerosols, for neutrally charged aerosols, there is an additional step. The charged fibers capture neutrally charged aerosols by dielectrophoresis. The first step is when the neutrally charged aerosol come close to the charged fibers for which an electrical dipole is induced on the neutrally charged aerosols. Subsequently, the dipole aerosol reoriented with the opposite charge side being attracted to the charged fiber, resulting in aerosol capture. The electrical force is of close-distance interaction, say on the order of several millimeters or less. The aerosol can come close distance to a nanofiber of  $0.3 \mu\text{m}$  diameter than a microfiber of  $6 \mu\text{m}$ , therefore resulting in stronger capture by dielectrophoresis.

## 1.2 Objectives

We have a few objectives to address in this study:

1. Does charged nanofiber filter work for real aerosols?
2. Does charged nanofiber filter exhibit a monotonic increase with increasing aerosol size similar to that of charged microfiber filter?
3. Can a charged nanofiber multiple-layer (multilayer) filter capture 100-nm ambient aerosols (simulating virus plus carrier) with 90% efficiency yet with low pressure drop  $\Delta p \leq 30\text{Pa}$  (3.1mm water)? For reference, a N95 respirator has at least 95% efficiency for 300 nm and with pressure drop  $\Delta p \leq 343\text{Pa}$  (35 mm water). It is well-

known that a user has difficulty in breathing through a mask or respirator having large pressure drop.

## 2. APPROACH

### 2.1 Electrospinning test setup

The nanofiber was developed using electrospinning using high voltage wherein a PVDF solution of appropriate consistency was injected through the syringe nozzle toward a substrate collector, see Fig. 2a. The syringe was charged at high voltage of 20 kV. As the electrical force exceeded the surface tension force, a Taylor cone formed at the tip of the syringe nozzle. The cone evolved into a fine filament streaming toward the collector. During the flight, both repulsion of like charges deposited on the fiber together with evaporation thinned out the fiber diameter. This is especially during the latter whipping motion of the jet. Once the fiber jet landed onto the substrate, the fiber diameter was reduced below 1  $\mu\text{m}$ , and typically 0.2 – 0.5  $\mu\text{m}$ . High quality nanofiber mat serving as a good filter can be formed free of beads and balls, which were remaining solution droplets that have yet been electrospun into nanofibers.

### 2.2 Filter charging

The filter mat with nanofibers was placed under a charging device under high voltage 10-30kV as shown in Fig. 2a. Fig. 2b shows a filter media charging set-up, which is also known as corona charging.

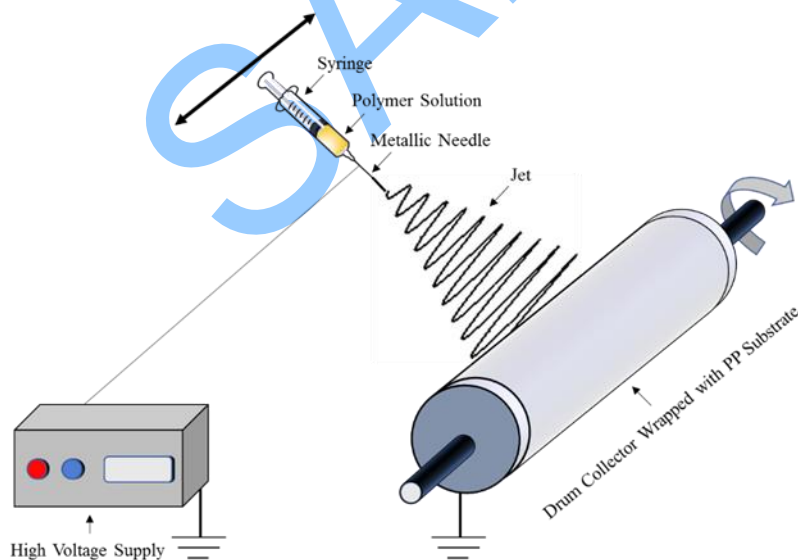


Fig. 2a – Electrospinning nanofibers using a syringe connected to a high voltage supply.

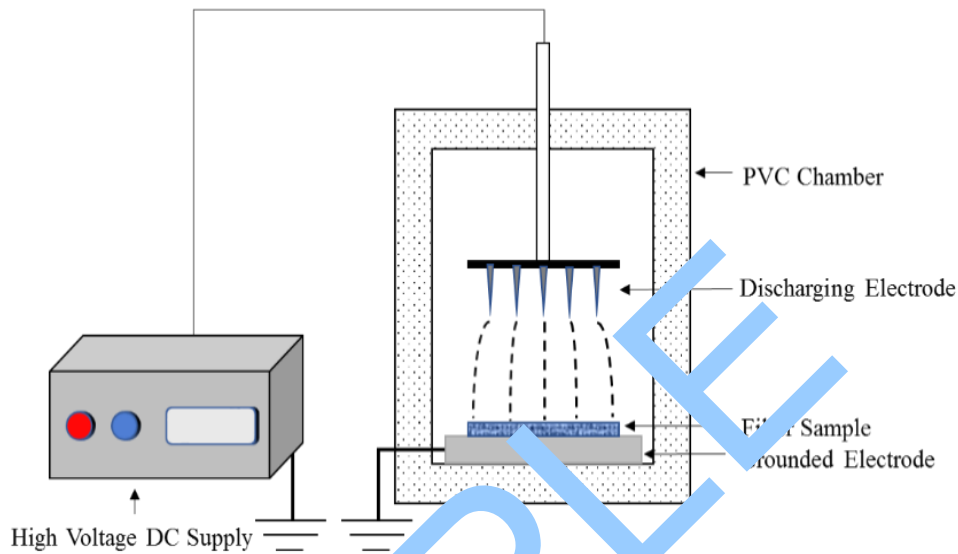


Fig. 2b – Corona discharge experimental setup.

### 2.3 Filter tester

A portable tester has been developed [3] as shown in Fig. 2c. Here, the filter tester consisted of two identical filter holders arranged in parallel to the incoming ambient air flow. Air was being sucked into the tester via a vacuum pump for which the feed rate of ambient air was controlled by the needle valve. Only one filter holder contained the test filter. First, the blank holder without the filter admitted incoming air from the surrounding. This was controlled by the two-way valve downstream of the filter holder. The flow rate of air was controlled by the suction from the vacuum pump and the needle valve. A slip stream of the airflow was sent to the portable aerosol mobility spectrometer (PAMS) that measured the feed size distribution of the slip stream. This corresponds to the aerosol concentration upstream of the test filter,  $C_u(D_p)$ . Subsequently, the two-way valve was switched back to allow air to flow through the filter holder that contained the test filter. The needle-valve of the pump was adjusted such that the flow rate was the same as that through the blank filter holder so that the same test velocity was maintained. Again, the aerosol size distribution of a slip stream of the downstream flow was measured by the PAMS. This corresponded to the aerosol concentration downstream of the test filter, i.e. concentration of the filtered stream  $C_d(D_p)$ . Subsequently, a third measurement was taken on the blank filter again to monitor the aerosol concentration upstream of the filter. The average of the first and third measurements represented the feed concentration  $C_u(D_p)$  such that any variations during the measurement period within 10 min could be minimized.

Thus, the filter grade efficiency  $\eta(D_p)$  can be inferred from the following equation,

$$\eta(D_p) = 1 - \frac{c_d(D_p)}{c_u(D_p)} \quad (1a)$$

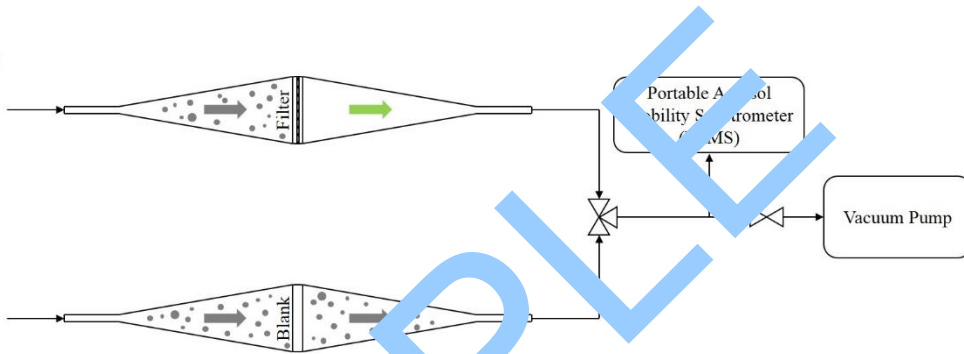


Fig. 2c – Portable test rig for measuring unfiltered and filtered air, respectively, from the ambient. The ambient aerosols were taken from a spot 30 m from a busy road leading to the cross-harbor tunnel where aerosols consisted of both traffic pollutants and smog particles [21] from photochemical oxidation near the harbor.

### 3. RESULTS, INTERPRETATIONS AND DISCUSSIONS

#### 3.1 Nanofiber morphology

Fig. 3a shows an image on the PVDF nanofibers obtained from the scanning electron microscope (SEM). Fig. 3b shows the fiber diameter distribution by counting over 100 fibers from 3 to 4 different small samples extracted from the filter. The size distribution was Gaussian with the mean size at  $525 \pm 191$  nm.

On the other hand, a typical ambient aerosols size distribution as measured by the portable filter test rig is shown in Fig. 3c. The mode (size with the maximum number) was about 83 nm, which was less than 100 nm; therefore, the ambient feed was considered as nanoaerosols.

#### 3.2 Ambient aerosol testing

For a 6-layer charged filter, Fig. 4 shows the grade efficiency of aerosol capture for different aerosol size on the abscissa scale, which is cast in logarithmic scale. In Fig. 4, there are two sets of data and two corresponding curves. The symbols represent test measurements while the continuous curve theoretical prediction [1]. The lower data set and curve correspond to mechanical capture of uncharged filter without dielectrophoresis, while the upper data set and curve the combined dielectrophoretic and mechanical capture of charged filter. Several comments can be made. First, the test data agree with the prediction reasonably well for the combined effects, whereas the agreement is only “approximate” for the mechanical capture as there is quite a bit of scatter in the data. The combined mechanical and dielectrophoresis capture is higher than just with mechanical capture. In both cases, there is a minimum particle

efficiency corresponding to a maximum particle penetration size (MPPS). The MPPS for the mechanical capture is about 150 nm while that with the dielectrophoresis added is about 80 nm. The latter is due to the added dielectrophoretic capture that favors the larger aerosols, which shifts the MPPS to a smaller aerosol size. The pressure drop of the filter  $\Delta p$  versus fiber basis weight  $W$  ( $\text{g}/\text{m}^2$ ) is shown in Fig. 5. The  $\Delta p$  of the multilayer filter increases linearly with the fiber basis weight due to maintain constant fiber packing density  $\alpha$  while that of the single layer filter increases nonlinearly with the fiber basis weight with increasing  $\alpha$  [1]. For a given  $W$ , especially for  $W > 3 \text{ g}/\text{m}^2$ , the  $\Delta p$  of the multilayer filter is lower as compared to that of the single layer filter. This is a key advantage of the multilayer filter, having lower pressure drop or flow resistance.

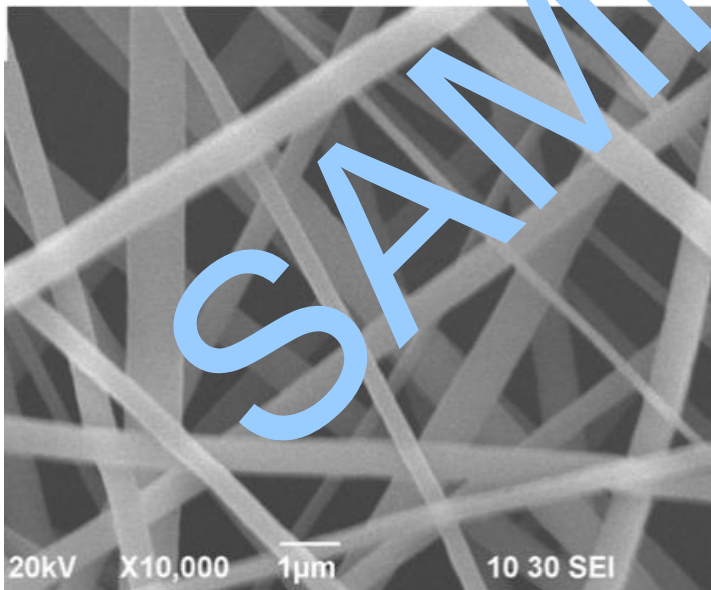


Fig. 3a – SEM image of PVDF nanofibers.

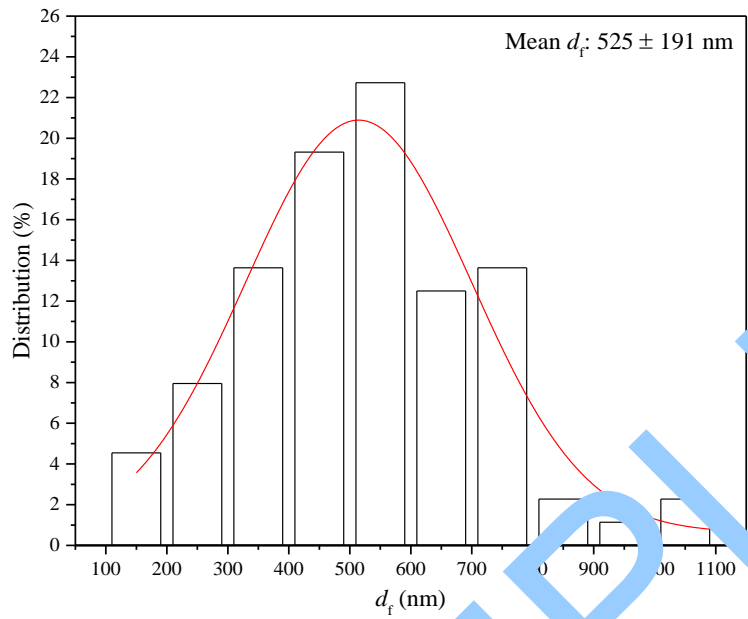


Fig. 3b – Distribution of nanofiber diameter, with mean fiber diameter  $525\text{nm} \pm 191\text{nm}$ .

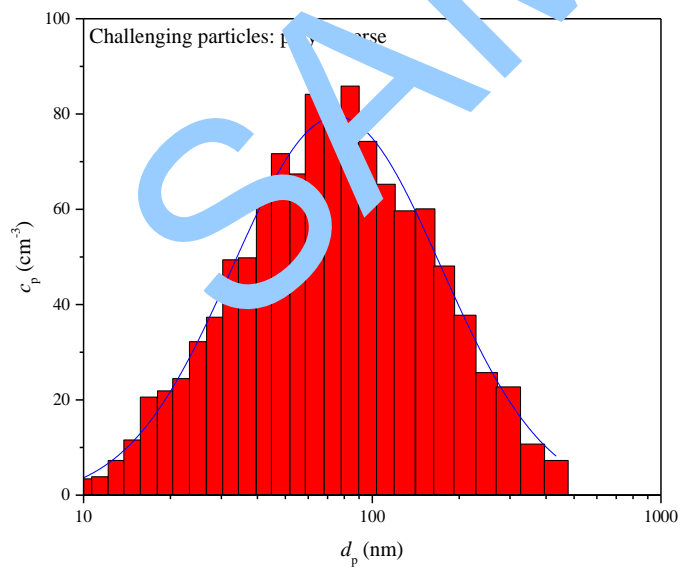


Fig. 3c - Typical size distribution of aerosols detected by inner condensation particle counter of PAMS of ambient aerosols with median at 75 nm.



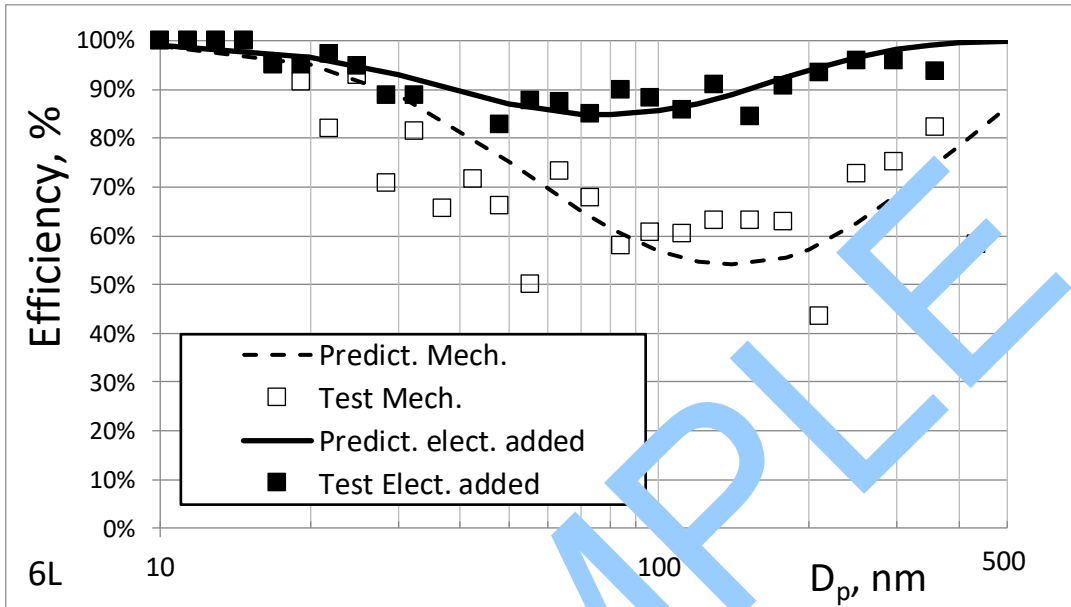


Fig. 4 – Grade efficiency versus aerosol size for 6-layer (6L) filter.

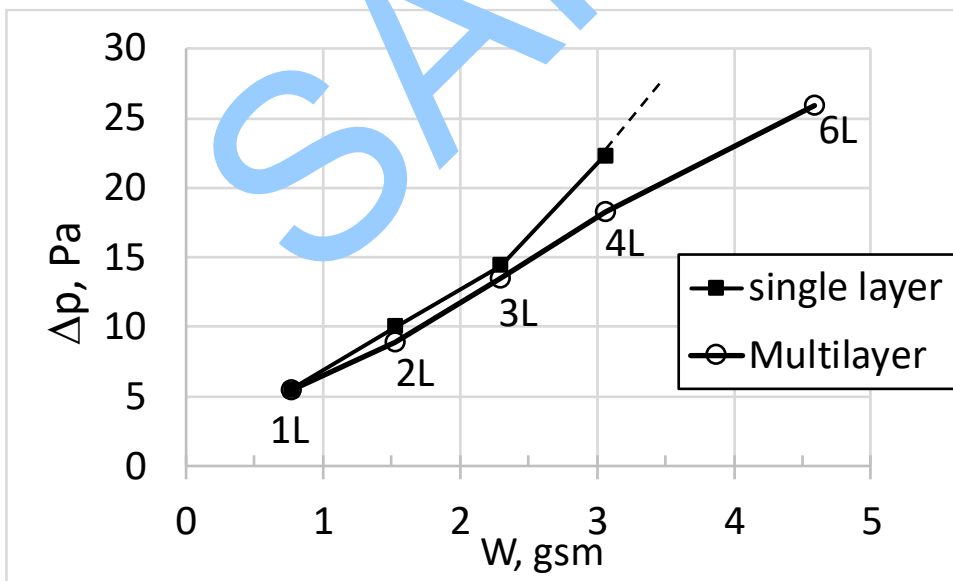


Fig. 5 – Pressure drop comparison between single and multi-layer filters.

The benefit-to-cost ratio is determined by the quality factor ( $QF$ ) as defined by

$$QF = -\ln(1 - \eta) / \Delta p \quad (2)$$

During the increase of fiber basis weight,  $QF$  often drops as the efficiency increases only marginally while the pressure drop increases substantially. Higher pressure drop means higher operating power to drive flow through the filter as power is the product of flow rate and pressure drop. Even for use in personal protection, it is highly desirable to maintain constant  $QF$  with higher efficiency inferring better protection. The relationship between efficiency for a given aerosol size capture and pressure drop associated with the filter for constant  $QF$  can be obtained by rearranging Eq. 2,

$$\eta = 1 - \exp(-QF\Delta p) \quad (3)$$

Figs. 6-8 show respectively the efficiency of 55-, 100- and 300-nm aerosols as function of pressure drop for constant  $QF$  curve (or iso- $QF$  curve) of 0.1, 0.13 and 0.15/Pa, respectively. Referring to Fig. 6 for the 55-nm ambient aerosols, the efficiency increases with more layers, 2L to 4L, at constant  $QF=0.1/\text{Pa}$ . With 6L, the  $QF$  drops slightly below 0.1/Pa. With a pressure drop of 26 Pa, the efficiency for the 55-nm aerosol for the 6L filter is 88%. Referring to Fig. 7 for the 100-nm ambient aerosols, the efficiency increases with more layers, 2L to 4L, at constant  $QF=0.1/\text{Pa}$  as with the 55-nm aerosol case. With 6L, the  $QF$  drops slightly below 0.1/Pa. With both 1L and 6L, the efficiency drops off as compared to those corresponding to the iso- $QF$  curve for 0.1/Pa. With the filter pressure drop at 26 Pa, the efficiency for the 100-nm aerosol for the 6L filter is 88%. Similar remarks can be made for the 300-nm aerosol as shown in Fig. 8. In fact, the  $QF$  test data are slightly higher than those indicated by the iso- $QF$  curve at 0.1/Pa for the 300-nm aerosols. For the 6L filter, at 26Pa, the efficiency for the ambient aerosol reaches 96%!

### 3.3 Sodium chloride aerosol testing

It is of interest to compare the efficiency of the ambient aerosol as compared to those of the sodium chloride (NaCl) aerosols, which is a standard test aerosol for measuring the N-type respirators (e.g., N-95, FFP2, KN95). The test of NaCl aerosols requires an aerosol source generated by a submicron aerosol generator (SMAG) and a differential mobility particle analyzer (DMA) upstream of the test filter, see Chapter 4 [1]. Fig. 6 shows that when the efficiency of the 50-nm aerosols is plotted against pressure drop. It gives similar behavior as that of the ambient aerosols. However, for a given pressure drop or fiber basis weight of the filter, the efficiency is 4-10% higher! This is clearly seen in Fig. 6. For the 4L filter, the efficiency for the ambient and NaCl aerosols is 80% and 89%, respectively, while for the 6L filter they are 88% and 92%, respectively. Similar behavior can be seen in Fig. 7 for the 100-nm aerosols and Fig. 8 for the 300-nm aerosols. In fact, at 26 Pa pressure drop the efficiency attains 94% in Fig. 8 for the 100-nm NaCl aerosol, while the efficiency attains 98% in Fig. 9 for the 300-nm NaCl aerosols! Therefore, the filter can be considered having spec equivalent to a "N98" even though N98 respirator does not exist in the test standard. In the same figure, the capture of 300-nm ambient aerosols is at 96%, which is only 2% less than that of the NaCl aerosols.

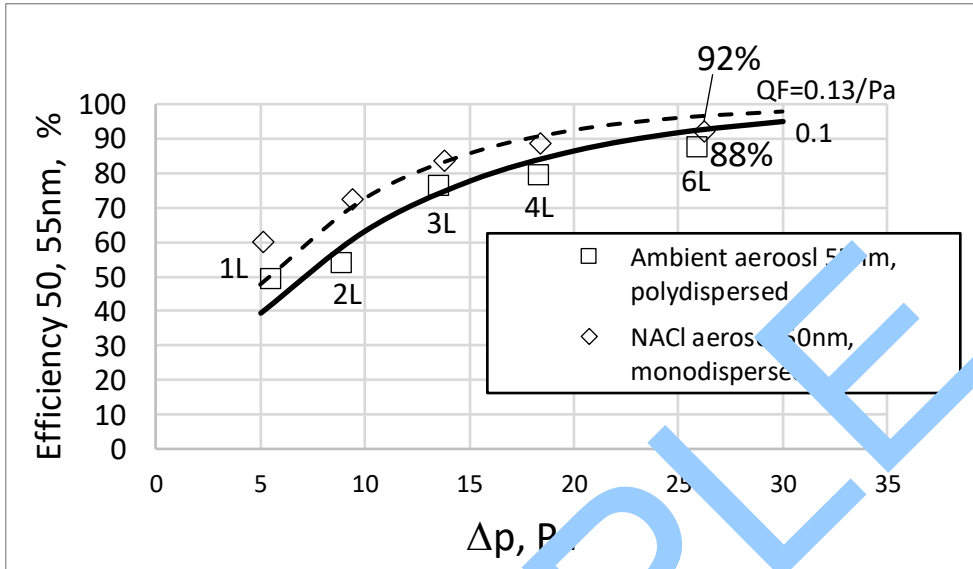


Fig. 6 – 55-nm ambient aerosol with polydispersed size distribution versus 50-nm monodispersed NaCl aerosol challenging the filter both at 5.3 cm/s.

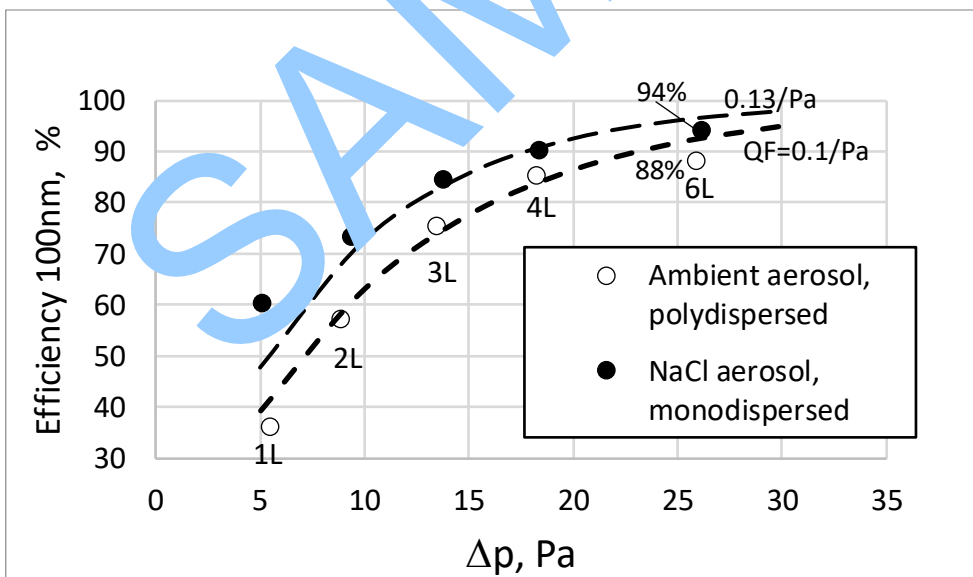


Fig. 7 – 100-nm ambient aerosol with polydispersed size distribution versus 100-nm monodispersed NaCl aerosol challenging the filter both at 5.3 cm/s.

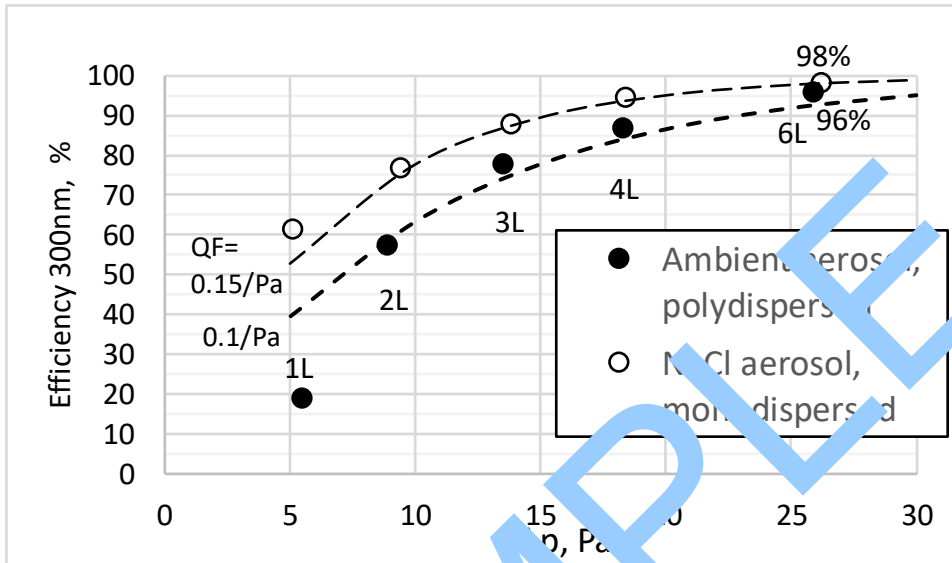


Fig. 8 – 300-nm ambient aerosol with polydispersed size distribution versus 300-nm monodispersed NaCl aerosol capture efficiency in the filter, with both at 5.3 cm/s.

#### 4. CONCLUSION

Based on the foregoing discussion, PVDF nanofiber filter can be electrostatically charged and the resulting charged filter can effectively capture ambient aerosols. The larger aerosol size above 100 nm are better captured by the charged filter. The capture efficiency curve exhibits a minimum MPPS at 80 nm in the nanoaerosol size range with aerosols above this size having monochronic increase in efficiency due to electrical, interception and inertial impaction capture. Below this MPPS, the capture is primarily due to diffusion. Charged multilayer can capture ambient aerosol simulating airborne aerosol carrying virus. The charged filter can achieve 88% efficiency (close to our target of 90% efficiency for 100 nm) with  $\Delta p=26$  Pa which is less than 30 Pa (3.1mm water). For the 300-NaCl aerosols, 98% efficiency can be achieved with  $\Delta p =26$  Pa which is significantly below the limit of 343 Pa (35 mm water) specification of the N95 respirator.

#### ACKNOWLEDGEMENTS

The author wants to thank The Hong Kong Polytechnic University in supporting his travel to San Diego, CA, USA.

## REFERENCES

- [1] Wallace Woon-Fong Leung, Nanofiber filter technologies for filtration of submicron aerosols and nanoaerosols. Elsevier, 2021. Amsterdam, The Netherlands, Paperback ISBN: 9780128144687, eBook ISBN: 9780323859851.
- [2] N. Zhu et al., A Novel Coronavirus from Patients with Pneumonia in China, 2019, The New England Journal of Medicine, DOI: 10.1056/NEJMoa2001017, January 24, 2020.
- [3] WWF Leung, Yuen Ting Chiu, Experiments on filtering nano-aerosols from vehicular and atmospheric pollutants under dominant diffusion using nanofiber filter, Separation and Purification Tech. J., 213, 186-198, 2019.